

Production of ^{18}F , ^{22}Na , and ^{24}Na from Separated Isotopes of the Light Elements with 300- and 400-MeV Protons*

RALPH R. KORTELING†

*Department of Chemistry, Carnegie-Mellon University, Pittsburgh, Pennsylvania 15213 and
Simon Fraser University, Burnaby 2, British Columbia, Canada*

AND

ALBERT A. CARETTO, JR.

Department of Chemistry, Carnegie-Mellon University, Pittsburgh, Pennsylvania 15213

(Received 19 May 1969)

Cross sections for the production of ^{18}F , ^{22}Na , and ^{24}Na have been determined from the separated isotopes of magnesium, silicon, and sulfur, using 300- and 400-MeV protons. These values, together with previous measurements, provide data for targets of each mass number of 23 to 34 inclusive for ^{18}F and ^{22}Na and from 25 to 34 inclusive for ^{24}Na . The main feature of the results is that the cross section is highest for those targets having the N/Z closest to that of the products. Thus, events involving the loss of about the same number of neutrons as protons have the highest probability. Cascade-evaporation calculations were performed for 400-MeV protons on each of these nuclides. The calculations reproduce the experimental trends.

INTRODUCTION

THE production of ^{22}Na and ^{24}Na from elements with atomic numbers between 12 and 50, with 400-MeV protons has recently been reported.¹ The dominant feature of these results is the exponential decrease in cross section with increasing atomic number of the target, Z_T , or neutron number, N_T , for values of $Z_T \leq 30$ and $N_T \leq 41$. Above these values of Z_T and N_T abrupt discrepancies from this exponential trend have been observed. It is not clear as to the origin of these discrepancies. However, the possibility of target impurities can be ruled out on the basis of the excitation functions which have been observed.²

The exponential trend was compared with the behavior which might be predicted on the basis of the cascade-evaporation model of high-energy interactions. It was observed that the scatter in the cross sections, around the general descending exponential dependence, was removed or at least substantially reduced by dividing the experimental cross sections by the quantity (dN/dZ) . This quantity is the slope, on an N -versus- Z plot of the line connecting the average value of Z_T , N_T in naturally occurring elements and the locus of the product (Z_p, N_p) .¹

Since the cross section for these products appeared to be a strong function of the nucleon composition of the targets for $Z_T \leq 20$, it seemed desirable to obtain cross sections for the production of these products from a number of separated isotopes of the light elements. Thus, the production cross sections for ^{24}Na were meas-

ured from all the stable isotopes between ^{24}Mg and ^{34}S inclusive and for ^{18}F and ^{22}Na from all the stable isotopes between ^{23}Na and ^{34}S , inclusive, at 300 and 400 MeV. In this way, the variation of production cross section versus the target neutron and proton number could be examined in detail.

Dostrovsky *et al.*³ have proposed that the production of light fragments, which might include ^{24}Na , is predominantly controlled by the evaporation step of the high-energy interaction. Porile and Tanaka^{4,5} have shown by Monte Carlo cascade-evaporation calculations that the yield of ^{24}Na from copper is consistent with the general cascade-evaporation mechanism. However, others⁶ have inferred that some type of direct interaction is not inconsistent with their ^{24}Na product recoil measurements. The exact nature of the high-energy process by which products such as ^{24}Na are produced is in doubt. Evaporation calculations by Hudis⁷ appear to give consistent isobaric yield distributions for $^{24}\text{Na}/^{22}\text{Na}$ ratios. The comparison of the production probability as the target composition is changed one nucleon at a time should also help to answer some of these questions.

EXPERIMENTAL PROCEDURE

These experiments were performed in a manner similar to that in the previous studies.^{1,2} The internal beam of the Carnegie-Mellon University 440-MeV synchrocyclotron was used for the irradiations. Proton energies of 300 and 400 MeV were selected and are believed to be accurate to within ± 10 MeV.

* Work sponsored by the U.S. Atomic Energy Commission and the National Research Council of Canada.

† Present address: Simon Fraser University, Burnaby 2, British Columbia, Canada.

¹ R. G. Korteling and A. A. Caretto, *J. Inorg. Nucl. Chem.* **29**, 2863 (1967).

² R. G. Korteling and A. A. Caretto (unpublished).

³ I. Dostrovsky, R. Davis, Jr., A. M. Poskanzer, and P. L. Reeder, *Phys. Rev.* **139**, B1513 (1965).

⁴ N. T. Porile and S. Tanaka, *Phys. Rev.* **137**, B58 (1965).

⁵ N. T. Porile and S. Tanaka, *Phys. Rev.* **135**, B122 (1964).

⁶ V. P. Crespo, J. M. Alexander, and E. K. Hyde, *Phys. Rev.* **131**, 1763 (1963).

⁷ J. Judis and S. Tanaka, *Phys. Rev.* **171**, 1297 (1968).

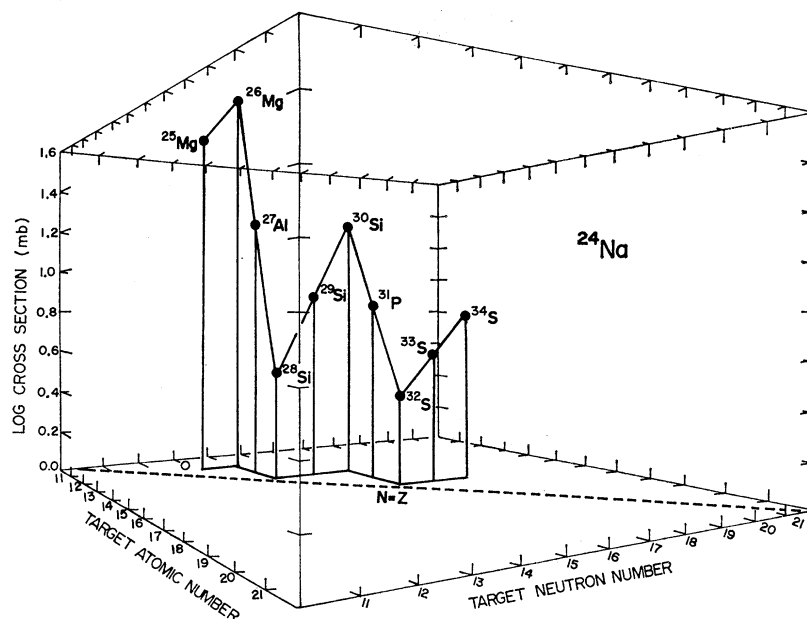


FIG. 1. Perspective representation of the cross section for the production of ^{24}Na at 400 MeV versus the neutron and atomic numbers of the target. The open circle on the $N-Z$ plane is the location of the product ^{24}Na . (Logarithms are to base 10.)

The characteristics of the targets are listed in Table I. All the target materials were supplied by Oak Ridge National Laboratory and the percent abundances are listed in Table II. The targets were prepared by mixing the separated isotopes of the various elements with spectroscopically pure boric acid and then compressing the mixture into uniform self-supporting pellets by means of a special die and a hydraulic press. Pressures of around 45 tons per sq. in. were suitable to prepare sturdy target pellets. These pellets were mounted on a probe head together with the aluminum monitor foils and Mylar guard films in the following order: 3-mil Al guard foil, 1-mil Al (99.99%) monitor, 3-mil Mylar guard film, target pellets, another Mylar guard film, and then another set of Al monitor foils. Two pellets, separated by 3-mil Mylar, were bombarded at the same time giving a mass of 200–300 mg/cm² for the total stack. Special care was taken to maintain alignment of the stack which was checked experimentally by comparing the activity of the front and back aluminum

TABLE I. Target characteristics.

Target	Form	Composition
^{24}Mg	Pellet	97% H_3BO_3 , 3% ^{24}MgO
^{25}Mg	Pellet	98% H_3BO_3 , 2% ^{25}MgO
^{26}Mg	Pellet	98.5% H_3BO_3 , 1.5% ^{26}MgO
^{27}Al	Foil	Metallic
^{28}Si	Pellet	98% H_3BO_3 , 2% $^{28}\text{SiO}_2$
^{29}Si	Pellet	98% H_3BO_3 , 2% $^{29}\text{SiO}_2$
^{30}Si	Pellet	98% H_3BO_3 , 2% $^{30}\text{SiO}_2$
^{32}S	Pellet	99.2% H_3BO_3 , 0.8% ^{32}S
^{33}S	Pellet	99.6% H_3BO_3 , 0.4% ^{33}S
^{34}S	Pellet	99% H_3BO_3 , 1% ^{34}S

monitor foils. The two activities generally agreed to within 1% of each other and very rarely exceeded 3%. An average number was taken for a beam measurement. The proton beam was monitored by the $^{27}\text{Al}(p, 3pn)^{24}\text{Na}$, $^{27}\text{Al}(p, 3p3n)^{22}\text{Na}$, and $^{27}\text{Al}(p, 5p4n)^{18}\text{F}$ reactions. Values for the cross sections of these reactions are those suggested by Cumming⁸ and are listed in Table III.

The irradiated pellets were mounted for counting without radiochemical separation. The ^{24}Na activity was counted by detecting the 2.76-MeV γ transition with 3×3-in. NaI(Tl) crystals coupled to multichannel analyzers. The ^{22}Na activity was determined by detect-

TABLE II. Composition of separated isotope targets (%).

Target nuclide	Composition			
	^{24}Mg	^{25}Mg	^{26}Mg	
^{24}Mg	99.96	0.03	<0.02	
^{25}Mg	0.39	99.21	0.4	
^{26}Mg	0.16	0.06	99.78	
		Silicon		
		^{28}Si	^{29}Si	^{30}Si
^{28}Si	99.38	0.37	0.25	
^{29}Si	4.36	95.28	0.36	
^{30}Si	32.3	2.7	65.0	
		Sulfur		
		^{32}S	^{33}S	^{34}S
^{32}S	98.1	0.3	1.5	0.1
^{33}S	36.96	61.15	1.89	<0.05
^{34}S	13.91	0.18	85.61	0.30

⁸ J. B. Cumming, Ann. Rev. Nucl. Sci. **13**, 261 (1963).

TABLE III. Production cross sections in mb.

Target	300-MeV protons				
	^{18}F	Product			^{24}Na
		^{22}Na			
^{23}Na	16.0 ± 0.50	a	37.7 ± 1.5	a	...
^{24}Mg	15.6 ± 0.20^b	(2) ^o	34.7 ± 0.2	(2)	$(0.13 \pm 5.00) \times 10^{-4}$ (2)
^{25}Mg	12.8 ± 0.17	(2)	19.1 ± 0.2	(2)	22.7 ± 0.75 (2)
^{26}Mg	7.92 ± 0.43	(2)	10.9 ± 0.2	(2)	29.2 ± 1.7 (2)
^{27}Al	6.6 ± 0.70	d	15.5 ± 1.6	d	10.1 ± 0.6 d
^{28}Si	9.64 ± 0.099	(2)	18.5 ± 0.1	(2)	4.32 ± 0.28 (2)
^{29}Si	5.66 ± 0.042	(2)	11.0 ± 0.1	(2)	7.17 ± 0.40 (2)
^{30}Si	5.09	(1)	5.71	(1)	11.1 (1)
^{31}P	3.51 ± 1.3	a	8.42 ± 0.92	a	5.53 ± 0.26 e
^{32}S	3.31 ± 0.003	(2)	7.86 ± 0.26	(2)	2.95 ± 0.22 (2)
^{33}S	2.33	(1)	5.35	(1)	4.25 (1)
^{34}S	1.61	(1)	2.69	(1)	3.19 (1)
400-MeV protons					
^{23}Na	17.95 ± 0.60	a	37.2 ± 1.00	e	...
^{24}Mg	18.2 ± 0.62^b	(3) ^o	33.5 ± 0.62	(3)	$(0.22 \pm 8.8) \times 10^{-3}$ (3)
^{25}Mg	14.0 ± 0.55	(3)	17.5 ± 0.76	(3)	24.1 ± 0.43 (3)
^{26}Mg	9.24 ± 0.22	(3)	9.86 ± 0.56	(3)	29.4 ± 1.2 (3)
^{27}Al	7.7	d	15.5	d	10.5 d
^{28}Si	11.2 ± 0.25	(3)	17.1 ± 0.68	(3)	4.36 ± 0.18 (3)
^{29}Si	7.31 ± 0.28	(3)	10.8 ± 0.14	(3)	7.73 ± 0.18 (3)
^{30}Si	7.50 ± 0.40	(3)	8.42 ± 0.07	(3)	13.10 ± 0.08 (3)
^{31}P	6.00 ± 1.0	a	9.39 ± 0.17	e	6.44 ± 0.35 e
^{32}S	5.00 ± 1.0	(3)	8.68 ± 1.50	(3)	3.30 ± 0.63 (3)
^{33}S	3.58 ± 0.42	(3)	4.86 ± 0.33	(3)	5.08 ± 0.40 (3)
^{34}S	3.40 ± 0.03	(3)	2.56 ± 0.26	(3)	6.11 ± 0.15 (3)

^a Reference 2.^b Standard uncertainty based on experimental precision.^o Number of replicate determinations.^d Reference 8.^e References 1 and 2.

FIG. 2. Perspective representation of the cross section for the production of ^{22}Na at 400 MeV versus the neutron and atomic numbers of the target. The open circle on the N - Z plane is the location of the product ^{22}Na . (Logarithms are to base 10.)

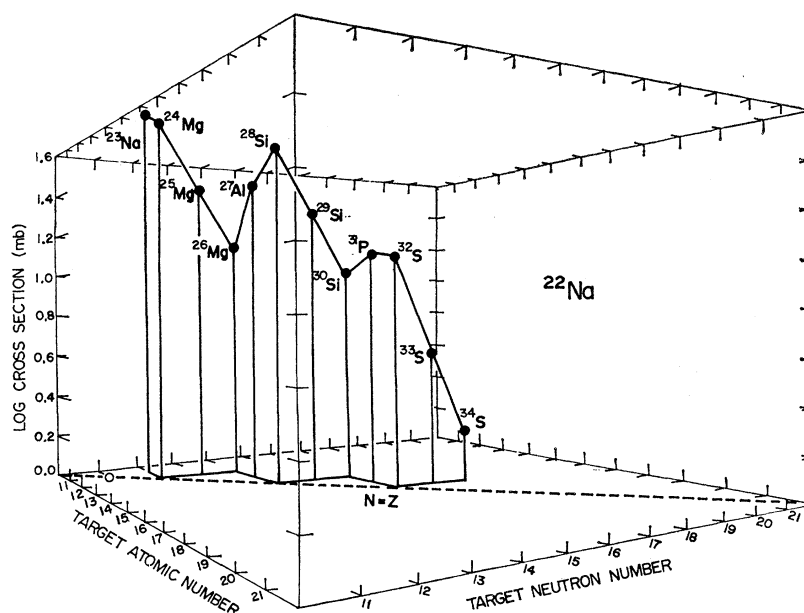


TABLE IV. Comparison of the cross sections from natural targets versus separated isotope targets.

Target element	300-MeV protons								
	$\sigma(^{18}\text{F})$, mb			$\sigma(^{22}\text{Na})$, mb			$\sigma(^{24}\text{Na})$, mb		
	Mg	Si	S	Mg	Si	S	Mg	Si	S
Separated isotope target ^a	14.5	9.31	3.22	30.5	17.8	7.62	5.66	4.66	2.97
Natural target	15.2	9.83	4.57	31.0	20.8	9.05	4.65	4.65	3.06
% difference	-4.7	-5.4	-34.7	-1.6	-14.4	-15.8	+19.6	+0.2	-2.9
Target element	400-MeV protons								
	Mg	Si	S	Mg	Si	S	Mg	Si	S
Separated isotope target ^a	16.8	10.9	4.92	29.2	16.5	8.39	5.90	4.79	3.43
Natural target	15.8	9.21	5.96	31.6	17.4	10.4	5.19	4.18	3.58
% difference	+6.1	+5.96	-19.1	-7.6	-5.2	-19.3	+12.8	+13.6	-4.3

^a Weighted cross sections based on natural abundances.

ing the annihilation radiation of the positron by 511–511-keV coincidence counting or by counting the 1.28-MeV γ with 3×3-in. NaI(Tl) crystals. The ^{18}F activity was determined by counting the annihilation radiation associated with its positron decay with a 511-511-keV coincidence counter. In order to decrease the ^{11}C contribution to the ^{18}F activity, the samples were generally allowed to decay for 4 h before initiating the measurements. The ^{18}F decay was then measured over a period of 8–12 h. During this time the decay curve exhibited the 110-min half-life of ^{18}F except for a slight 20-min component due to the ^{11}C contribution.

RESULTS

The experimental cross sections for the production of ^{18}F , ^{22}Na , and ^{24}Na from the separated isotopes of the light elements are given in Table III. The average value, standard uncertainty, and the number of determinations are listed.

Since the product of the reaction of interest and that of the monitor were the identical nuclide in each case, the number of uncertainties associated with these measurements is reduced. A nominal 3% uncertainty is assigned to the total activity measurements. However, in the case of the ^{18}F activities a serious source of error was the contribution to this activity from the $^{18}\text{O}(p, n)^{18}\text{F}$ reaction. This reaction has a substantial cross section⁹ at these energies. Also, the number of atoms of separated isotope in the target pellets was often only 5–6 times the number of ^{18}O atoms present. The ^{18}F activity was corrected for the contribution from ^{18}O by measuring the ^{18}F activity in pure boric acid as a function of both target thickness and beam energy. Values of this correction to the measured ^{18}F activities varied from ~10% for ^{24}Mg targets to ~80% for ^{33}S and ^{34}S targets.

Corrections were applied for the contribution to the cross section for any given reaction from the small abundance of other target isotopes still in the enriched

material¹⁰ (Table II). As a test for the over-all uncertainty that these results are subject to, a comparison was made of the ^{24}Na , ^{22}Na , and ^{18}F cross sections from natural targets^{1,2} and the cross sections from the separated isotopes, appropriately weighted according to the natural abundances. The results of this comparison are presented in Table IV.

In addition to these uncertainties and errors, an additional 10–15% uncertainty in the experimental values is estimated due to target fabrication, misalignment, uncertainties in the percentage composition of the separated isotopes, uncertainties in the contribution from ^{18}O , and general experimental manipulations. Thus, the data have an over-all uncertainty of about 10–15%, which is in accord with the comparison presented in Table IV.

DISCUSSION

The data presented in Table II can be used to map out the ^{18}F , ^{22}Na , and ^{24}Na yield surfaces above the N -versus- Z plane. Figures 1–3 are perspective representations of these surfaces. In these figures the axis normal to the N - Z plane is $\log\sigma(\text{prod})$, the logarithm of the cross section for the production of ^{18}F , ^{22}Na , or ^{24}Na , and the points are plotted at the N and Z of the target.

The yield surface of ^{24}Na (Fig. 1) indicates that the cross section is a maximum for the most neutron excessive targets, and decreases as the N/Z of the target approaches unity. The N/Z of ^{24}Na is 1.18. Peaks in the ^{24}Na cross section occur for $^{26}\text{Mg}(N/Z=1.17)$, $^{30}\text{Si}(N/Z=1.14)$, and $^{34}\text{S}(N/Z=1.12)$. In each case, not counting the incident proton, equal numbers of neutrons and protons must be removed from these targets in order to produce ^{24}Na . For example, from ^{26}Mg targets a loss of one proton and one neutron is required. Similarly a loss of, respectively, three protons and three neutrons from ^{30}Si and five protons and five

⁹ A. A. Caretto, Jr., Report No. NYO-10693, 1964 (unpublished).

¹⁰ Composition and purity as given by Oak Ridge National Laboratory, supplier of separated isotopes.

FIG. 3. Perspective representation of the cross section for the production of ^{18}F at 400 MeV versus the neutron and atomic numbers of the target. The open circle on the N - Z plane is the location of the product ^{18}F . (Logarithms are to base 10.)

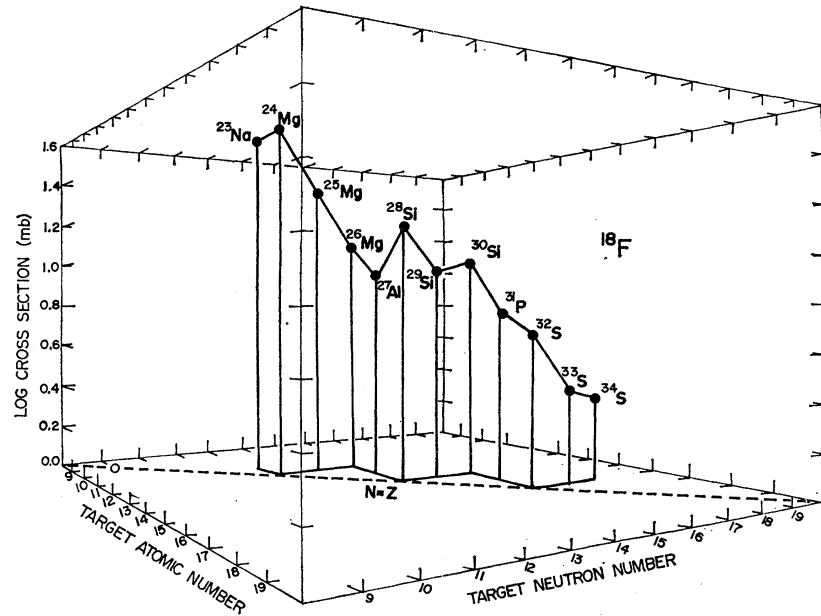
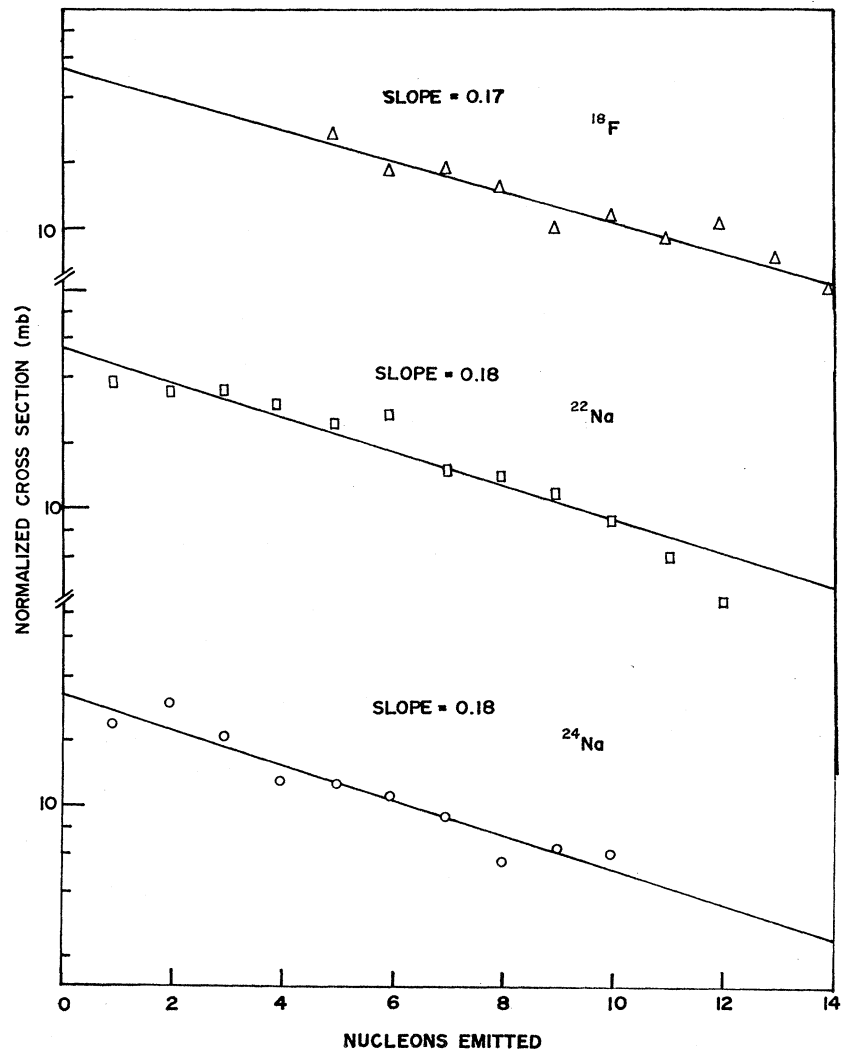


FIG. 4. Normalized production cross sections with 400-MeV protons versus the number of emitted nucleons to produce the product from the target. The normalization factor is explained in the text.



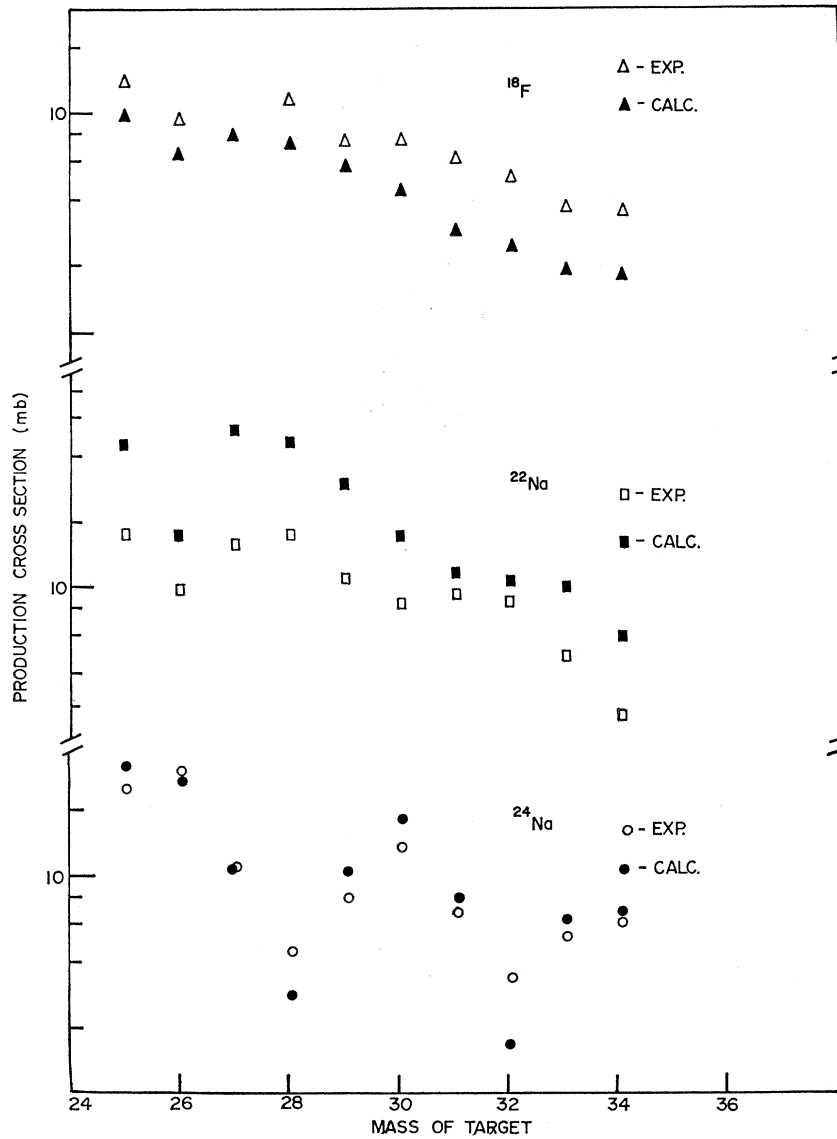


FIG. 5. Comparison of experimental production cross sections with values calculated by Monte Carlo calculations at 400 MeV.

TABLE V. Comparison of Monte Carlo cascade-evaporation calculations with experimental values at 400 MeV.

Target	^{18}F			^{22}Na			^{24}Na		
	σ_{calc}	$\sigma_{\text{calc}}/\sigma_{\text{expt}}$	σ_{expt}	σ_{calc}	$\sigma_{\text{calc}}/\sigma_{\text{expt}}$	σ_{expt}	σ_{calc}	$\sigma_{\text{calc}}/\sigma_{\text{expt}}$	σ_{expt}
^{25}Mg	9.56	0.68	14.0	47.0	2.69	17.5	31.5	1.31	24.1
^{26}Mg	6.38	0.69	9.24	17.1	1.73	9.86	26.4	0.90	29.4
$^{27}\text{Al}^a$	7.87	1.02	7.7	51.8	3.34	15.5	10.3	0.98	10.5
^{28}Si	7.02	0.63	11.2	45.8	2.68	17.1	2.72	0.62	4.36
^{29}Si	5.62	0.77	7.31	29.7	2.75	10.8	10.1	1.31	7.73
^{30}Si	4.33	0.58	7.30	17.4	2.07	8.42	18.1	1.38	13.10
^{31}P	2.78	0.46	6.00	11.7	1.25	9.39	7.50	1.16	6.44
^{32}S	2.40	0.48	5.00	10.6	1.22	8.68	1.64	0.50	3.30
^{33}S	1.89	0.53	3.58	10.1	2.08	4.86	6.01	1.18	5.08
^{34}S	1.76	0.52	3.40	5.93	2.32	2.56	6.80	1.11	6.11
Average of ratio		0.64			2.22			1.04	

^a Normalized $r_0=1.53$ to give best results with monitor cross sections.

TABLE VI. Characteristics of ^{24}Na production.

Target	Number of emitted nucleons	Average number of evaporated nucleons	% total	Average E^* of residual nuclei	Average E^* per evaporated nucleon
^{25}Mg	1	0.16	0.16	7.75	
^{26}Mg	2	0.95	0.48	17.75	18.69
^{27}Al	3	1.45	0.48	27.84	19.20
^{28}Si	4	2.25	0.56	37.80	16.80
^{29}Si	5	3.73	0.75	29.91	8.02
^{30}Si	6	4.46	0.74	35.27	7.91
^{31}P	7	4.80	0.69	41.87	8.72
^{32}S	8	5.53	0.69	52.94	9.57
^{33}S	9	7.17	0.80	57.17	7.97
^{34}S	10	7.65	0.77	62.28	8.14
^{35}Cl	11	8.63	0.78	71.06	8.23
^{46}Sc	21	16.5	0.79	127.63	7.74

neutrons from ^{34}Si is required to produce ^{24}Na . The products ^{18}F and ^{22}Na lie essentially on the line of stability. Figures 2 and 3 indicate that the maximum cross section for these products occurs for targets closest to the line of stability. These targets are again those requiring the loss of the same number of protons as neutrons.

This experimental behavior suggests the empirical relationship which has been used before¹ of dividing the experimental cross sections by the quantity (dN/dZ) to correct for unequal emission of neutrons and protons where dN/dZ is the slope on an N -versus- Z plot of the line connecting the target and product. Figure 4 displays the data in this normalized form. The lines drawn through the points are the best fits and show a remarkable similarity in magnitude and slope independent of final product. This result suggests that a statistical emission of nucleons is the dominant feature of these reactions.

Monte Carlo cascade and evaporation calculations were performed on each of the stable nuclides ^{25}Mg through ^{35}Cl and also ^{46}Sc using 2000 incident protons at 400 MeV. The cascade calculations were performed using the Vegas program¹¹ adapted for use on the Univac 1108 of Carnegie-Mellon University. Both the STEP and STEP-NO versions of this program were employed. Both programs take into account the radial variations of the nuclear density by dividing the nucleus into seven concentric zones or steps of constant density. Refraction and reflections of the incident and cascade particles at the interfaces of these zones are included in the STEP version but not included in the STEP-NO version. The evaporation calculations employed a program adapted for the Univac 1108^{12,13} and patterned after that originally written by Dostrovsky *et al.*¹⁴ Evaporation cal-

culations were performed ten times on each residual nucleus resulting from the Vegas cascade calculation.

Cross sections for the production of the products were calculated from the cascade-evaporation results by the relation

$$\sigma_{\text{calc}} = \sigma_g (N/N_T),$$

where N was the number of events leading to the particular product, N_T was the total number of events, and σ_g was the geometric cross section. The value of the nuclear radius parameter was determined by optimizing the three monitor values and was found to be 1.53 F. There was no appreciable difference between the STEP and STEP-NO values but the STEP-NO results were found to give better values for the monitor cross sections and they are listed in Table V and displayed in Fig. 5.

The comparison of the calculated values with the experimental results shows that the trends in cross sections are reproduced and that the values for ^{24}Na are in general good agreement. However, the calculations tend to overestimate the values for ^{22}Na by a factor of 2 and underestimate the ^{18}F values by a similar factor. In general, the calculation seems to underestimate the length of the cascade-evaporation chain with the input parameters we used. A change of input parameters could possibly improve this over-all agreement, but no attempt was made to maximize the agreement in this way. The over-all agreement was considered to be satisfactory and the calculations to adequately represent the mechanism involved in these reactions.

The results of the calculations were sorted to identify the residual nucleus which, on evaporation, produced ^{24}Na . The atomic number, mass, and excitation energy of these residual nuclei were obtained for each case. This information is given in Table VI and displayed in Fig. 6 in terms of average values. It is interesting to note that when 5 or more nucleons are emitted to form the product, the evaporation contribution to the total reaction has essentially reached a constant value of 75–80%. At the same time, the average excitation

¹¹ K. Chen, Z. Fraenkel, G. Friedlander, J. R. Grover, J. M. Miller, and Y. Shimamoto, *Phys. Rev.* **166**, 949 (1968).

¹² F. M. Kiely, Ph.D. thesis, Carnegie Institute of Technology, Pittsburgh, Pa., 1967 (unpublished).

¹³ J. Urbon (private communication).

¹⁴ I. Dostrovsky, Z. Fraenkel, and G. Friedlander, *Phys. Rev.* **116**, 683 (1959).

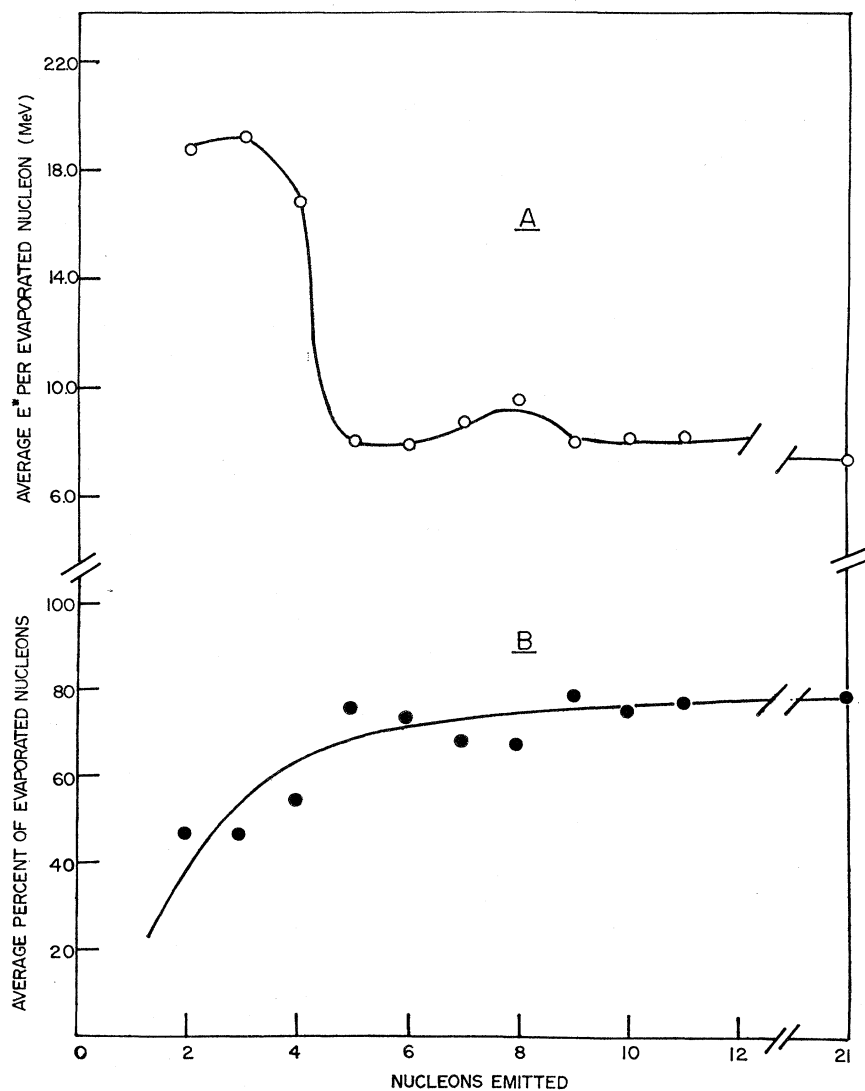


FIG. 6. Average values in the formation of ^{24}Na determined from the Monte Carlo calculations for 400 MeV. (A) Average excitation energy per evaporated nucleon of the residual cascade nuclei leading to the formation of ^{24}Na . (B) Average percentage of the cascade evaporation chain due to the evaporation process.

energy per emitted nucleon of the residual nucleus has also reached an approximate constant value of 8 MeV. In the cases where fewer nucleons were emitted, the cascade contribution is higher as is to be expected; however, the average excitation energy per nucleon necessary to produce the product by subsequent evaporation is dramatically higher, which was not expected. This effect possibly reflects the need to emit more protons than neutrons and the fewer channels available for the reaction. This explanation is consistent with the slight increase in the average value for the emission of 8 nucleons where in fact it is a $(5p, 3n)$ emission chain. The other emission chains with 5 or more emitted nucleons have a more even distribution of emitted protons and neutrons. In any case, when more than 5 or 6 nucleons are emitted to form the product, the calculation indicates that the evaporation step is the dominant process ($\sim 80\%$) and that an average of about 8 MeV of excitation energy per emitted nucleon is necessary.

CONCLUSIONS

The ratio of emitted neutrons to protons is an important aspect in the production of products in spallation reactions. The increased probability for the cases where the ratio is ≈ 1 suggests the prime importance of the statistical aspect of emitting nucleons in relation to considerations of binding energy, Coulomb barriers, etc. This behavior is reproduced in the Monte Carlo cascade-evaporation calculations, although the calculations did not agree in all details.

In analyzing the relative importance of the cascade and evaporation steps of the calculation for the production of ^{24}Na , it was found that by the time five or more nucleons have been emitted, average calculated quantities had reached approximate constant values. In particular, it was found that $\sim 80\%$ of the emission chain is due to the evaporation step and that ~ 8 MeV of excitation energy per evaporated nucleon was necessary. Deviations from these values occurred when

less than 5 nucleons were emitted or when the ratio of emitted neutron to protons varied greatly from ~ 1 .

ACKNOWLEDGMENTS

We wish to thank the operating crew of the Carnegie-Mellon University Nuclear Research Center for aid in

making the irradiations. We also thank Mrs. Christa Hombach Gaebel and Gary Smay for help in sample counting, computer assistance, and other miscellaneous help. We also extend our appreciation to John Urbon and Carol Kier for aid in performing the cascade-evaporation calculations.

PHYSICAL REVIEW C

VOLUME 1, NUMBER 1

JANUARY 1970

Photoexcitation of the 7.64-MeV Magnetic Dipole Levels in Cd^{112} and Ni^{62} by Iron Capture Gamma Rays*

G. P. ESTES†

Department of Nuclear Engineering, University of Virginia, Charlottesville, Virginia

AND

K. MIN

Department of Physics, University of Virginia, Charlottesville, Virginia and Department of Physics and Astronomy, Rensselaer Polytechnic Institute, Troy, New York 12181

(Received 22 July 1969)

The elastic and inelastic scattering of iron capture γ rays from the 7.64-MeV $M1$ levels in Cd^{112} and Ni^{62} were studied with a Ge(Li) spectrometer. Eleven energy levels in Cd^{112} and three in Ni^{62} observed in this experiment are compared with the levels excited in (d, p) experiments. Angular distribution measurements were made for four strong transitions in Cd^{112} and two in Ni^{62} , giving the following spin assignments: Cd^{112} : 0.62-MeV level (2), 1.23-MeV (0), 1.88-MeV (0), 7.64-MeV (1); Ni^{62} : 2.06-MeV (0), 7.64-MeV (1). In both nuclei, only the 0^+ member of the two-quadrupole phonon triplet (0^+ , 2^+ , 4^+) is strongly excited in this experiment, indicating very different components in the wave functions of the 0^+ and 2^+ members.

I. INTRODUCTION

THE nuclear fluorescence of neutron-capture γ rays is a relatively new method to study the individual nuclear levels near the neutron binding energies.^{1,2} Since resonance fluorescence preferentially excites the levels immediately below the neutron binding energy where the γ reemission is the only possible deexcitation mode, this type of experiment supplements the slow neutron spectroscopy which probes the individual nuclear levels above the neutron binding energy.

Some 50 different resonances involving the use of about 20 capture sources have been reported.³ In most cases, the spectra of the reasonably scattered photons were measured by a NaI detector. Because of its limited energy resolution and complex energy response, the detailed study of nuclear properties (energy, spin,

parity, and the radiation width) was usually confined to the scattering level. More recently, some of the previously observed resonances were restudied using either NaI spectrometers working in coincidence or a Ge(Li) spectrometer. These new measurements show that a resonant level excited by the neutron-capture γ rays has an appreciable branching to the lower excited states even though the ground-state transition seems to be generally the most dominant. The inelastic scattering of the neutron-capture γ rays thus provides a useful method to study the nuclear properties of the lower excited states. Of particular spectroscopic interest is the determination of nuclear spins of the excited states by angular distribution measurements of the inelastically scattered photons. The angular distribution of resonantly scattered photons is identical to that of two successively emitted γ rays,⁴ and the interpretation is made simple by the fact that the extreme monochromaticity of the incident capture γ rays insures that the resonance fluorescence is due to a single level.

The nuclear fluorescence of the 7.64-MeV iron capture γ rays in cadmium and nickel has been previously

* Work supported by the National Science Foundation.

† Atomic Energy Commission Special Fellow.

¹ C. S. Young and D. J. Donahue, *Phys. Rev.* **132**, 1724 (1963).

² G. Ben-David and N. Huelschmann, *Phys. Letters* **3**, 82 (1963).

³ G. Ben-David, B. Arad, J. Balderman, and Y. Schlesinger, *Phys. Rev.* **146**, 852 (1966).

⁴ D. R. Hamilton, *Phys. Rev.* **58**, 122 (1940).